AN INVESTIGATION INTO THE EFFECTS OF EXPERIMENTAL ERRORS ON THE CORRELATION BETWEEN FEA AND TEST RESULTS FOR A WELDED FUSELAGE PANEL

J. Shah, A. Gibson, M. Price
School of Aeronautical Engineering, Queen's University of Belfast, Belfast, UK

Abstract

Discrepancies between finite element (FE) predictions and experimental results for a welded fuselage panel subjected to uni-axial compression were investigated in order to determine the impact of experimental errors. To establish the extent to which these experimental errors can affect results, an investigation was carried out, centring on one particular welded specimen, which was tested and analysed previously. Finite element models, using shell elements and a combination of shell and solid elements, were generated to examine the effects of using various boundary conditions to represent the experimental set-up. A newer version of the software package ABAQUS also allowed for more accurate modelling of the panel shape. It was found that the newer version of ABAQUS produced better stiffness and failure load results. Also, the addition of solid elements to the FE model produced stiffness values that closely followed the experimental results.

1 Introduction

In recent years, much effort has been put into the development of FE modelling with respect to the analysis of aircraft fuselage panels, the overall goal being to replace conventional stressing methods. At QUB, research in this area has involved the modelling/analysis of flat riveted compression buckling and shear buckling panels, curved riveted compression buckling panels and flat welded compression buckling panels. In order to assess the validity of the modelling procedures and the accuracy of the predictions of strength and behaviour, an experimental programme has also been conducted in which the various types of panel mentioned above have been loaded to failure. This has allowed the comparison of FE predictions and test results, generally via load-displacement curves.

In some cases, especially for the welded specimens, there was less than satisfactory correlation between experimental results and FE predictions and it was thought that this was due largely to two aspects:

(i) the true shape of the specimen not being represented accurately in the model
(ii) differences in the boundary conditions assumed in the FE models and those applied in practice.

Whereas conventional analysis methods have a large margin built in for error, and are fine for design purposes, such uncertainty is not acceptable for FE methods. It is necessary to distinguish between physical effects and modelling idealisation errors. This study focuses on a specimen previously tested, which consisted of one blade stringer welded centrally to a skin panel. To ensure the top and bottom ends of the skin panel stayed perpendicular to the testing platen, they were cast in a low melting point alloy, Cerrobend. In addition, the sides of the panel were held in grooved steel bars. Figure 1 shows the configuration of the test panel. Dimensions are in inches [1]. The

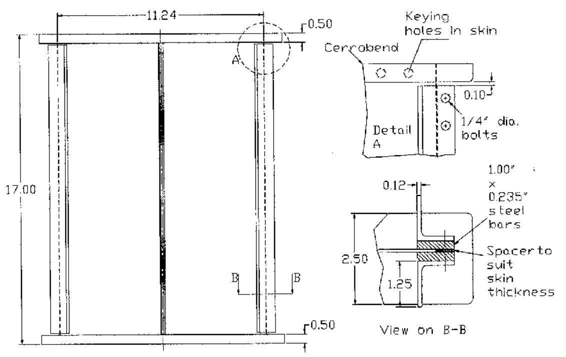

Figure 1. Panel geometry

panel was manufactured using Al 6013-T6 sheets. The skin had a nominal thickness of 0.125" and was mechanically milled down to 0.075" leaving a "pad-up" along the centreline as shown in Figure 2. The pad-up was used to shift the weld lines away from the working thickness of the skin.

Several revised models of the panel were analysed and the results compared to the original FE model and test results via load-displacement curves. First, a newer version of the software package, ABAQUS, was used for the revised models. This allowed the pad-up area to be modelled differently than had been done previously. Next the panel was analysed with various boundary conditions to represent the effects of the Cerrobend. Finally, solid elements with Cerrobend material properties were added to the model. Non-linear buckling analysis was performed on each of the models with the deformed shape applied as the first mode shape pre-determined by a linear eigenvalue buckling analysis. The amplitude of deformation was set at 10% of the skin thickness. In reality, the specimen was bowed longitudinally, the outer skin surface being convex. There was also angular distortion along the weld line.

2 Modelling Methods

2.1 Pad-up Area

As stated above, a major issue in the correlation of test results with FE results had to do with modelling the shape of the panel correctly. Previously FE models of the panel were analysed using ABAQUS version 5.8. This older version lacked the means to model the pad-up at the skin-stringer interface directly. Figure 2 shows the pad-up section of the skin-stringer interface.

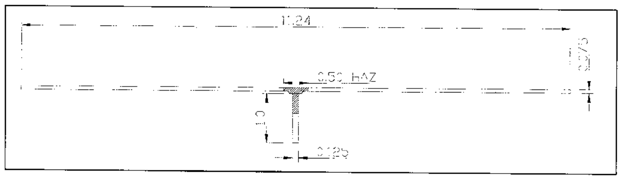

Figure 2. Panel cross-section

The panel was modelled using 8-noded quadratic shell elements. ABAQUS version 5.8 applied element properties such that the thickness was distributed evenly about the mid-surface. However, the mid-surface of the pad-up area is raised slightly above the skin mid-surface. Therefore, a dummy layer with negligible stiffness was placed beneath the skin to shift the neutral axis upward in the central welded section of the panel [2]. ABAQUS version 6.1, currently in use, allows the user to shift the neutral axis away from the mid-surface without creating a dummy material. Thus the shape of the panel is more accurately modelled.

2.2 Boundary conditions

Four sets of boundary conditions were applied simultaneously to the panel model:

(1) The base of the panel was constrained axially to represent a fixed condition.

(2) The sides of the panel were previously constrained in plane assuming simple support from the grooved steel bars. However, the new model assumed clamped conditions from the steel bars so that the side elements of the panel were constrained in plane and rotationally about the y-axis.

(3) The bottom and top rows of elements were constrained in plane and laterally to represent the effect of the Cerrobend.

(4) A compressive load was applied to the panel in the form of a displacement at the top row of nodes.

Figure 3 enlarges the left corners of the panel with applied boundary conditions.

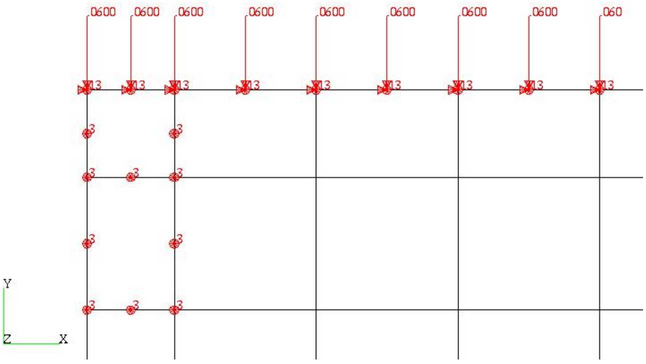

(a)

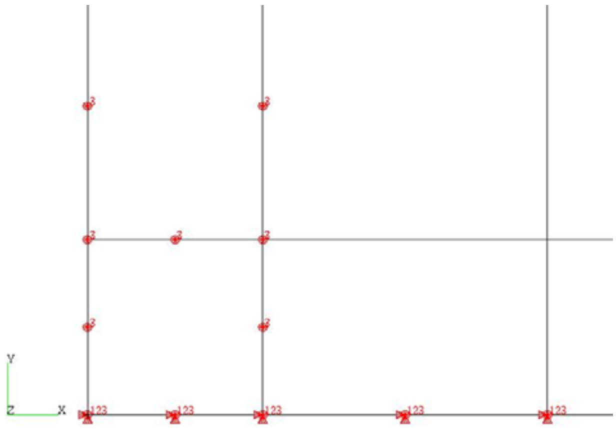

(b)

Figure 3. FE model with boundary conditions shown on (a) top left corner, and (b) bottom left corner

After completing analysis of this model, Cerrobend boundary conditions were changed to investigate the effect of constraining different lengths of the panel. Since the experimental skin panel exhibited lower stiffness than the FE model, the Cerrobend boundary conditions were reduced successively by rows of nodes until only the top row of nodes were constrained in plane.

2.3 Cerrobend

The models described above all assumed the Cerrobend effects were represented by appropriate boundary conditions. However, to thoroughly study the effect of Cerrobend on the panel, the FE model was now modified to represent realistic end conditions. Three-dimensional solid elements were built into the model that contained proper Cerrobend material properties.

Hexagonal 20-noded solid elements were placed directly on top of the panel's shell elements at the top and bottom half-inches of the welded panel. Tensile tests were carried out on three Cerrobend specimens in order to determine the mechanical properties of the material. Results were averaged to determine the elastic and plastic material properties. Figure 4 plots the stress-strain curve for Cerrobend.

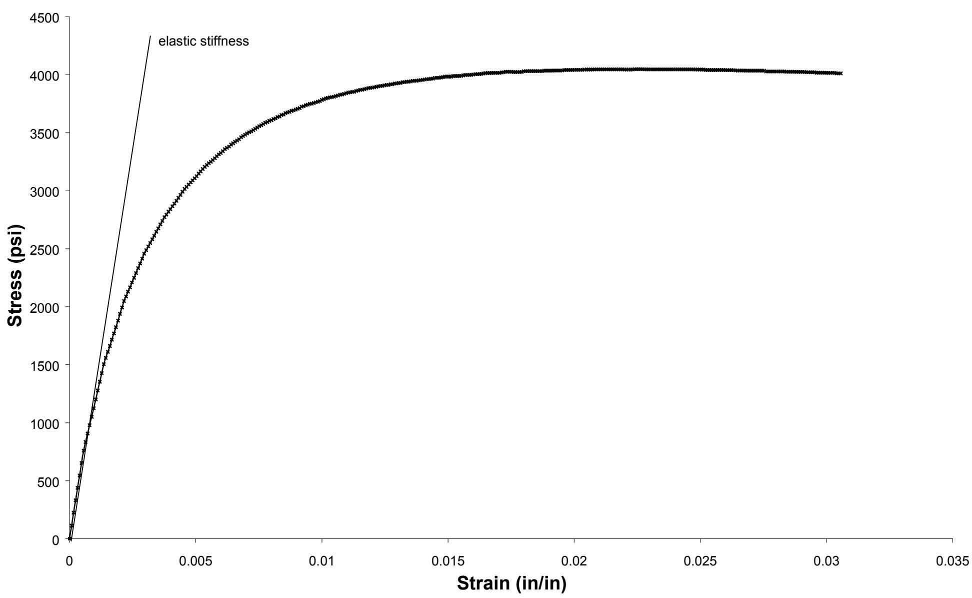

Figure 4. Stress-Strain curve of Cerrobend

The elastic modulus was found to be 1052000psi. In the plastic range, nominal stress and strain were converted to true stress and plastic strain using equations found in reference [3]:

$$\sigma_{true} = \sigma_{nom}(1 + \varepsilon_{nom}) \qquad (1)$$

$$\varepsilon_{pl} = ln(1 + \varepsilon_{nom}) - \sigma_{true}/E \qquad (2)$$

The Cerrobend material properties were then entered into the ABAQUS input file.

3 Results

3.1 Pad-up

Figure 5 shows the load-deflection curves for the experimental panel and two FE models analysed with different boundary conditions. The removal of the dummy layer in the analysis produces results that follow the experimental load-deflection curve more closely. Though the new model is less stiff with a lower failure load than previously predicted using ABAQUS version 5.8, FE results still over-predict stiffness. Nonetheless, the predicted failure load is lower than that measured experimentally, and consequently more conservative.

3.2 Boundary Conditions

After analysing the first model with boundary conditions mentioned above, Cerrobend constraints were changed to examine which boundary conditions most accurately represented the experimental panel's end conditions. Cerrobend constraints on the bottom and top rows of elements were relaxed in increments of one-quarter inch. As expected, constraining only the top and bottom rows of nodes reduced the panel stiffness, thus bridging the gap between FE and experimental results. Nevertheless, the FE model still over-estimated stiffness. Constraining only the top and bottom rows of nodes resulted in analysis that predicted a failure load matching the experimental value more closely, although it occurred at a greater displacement.

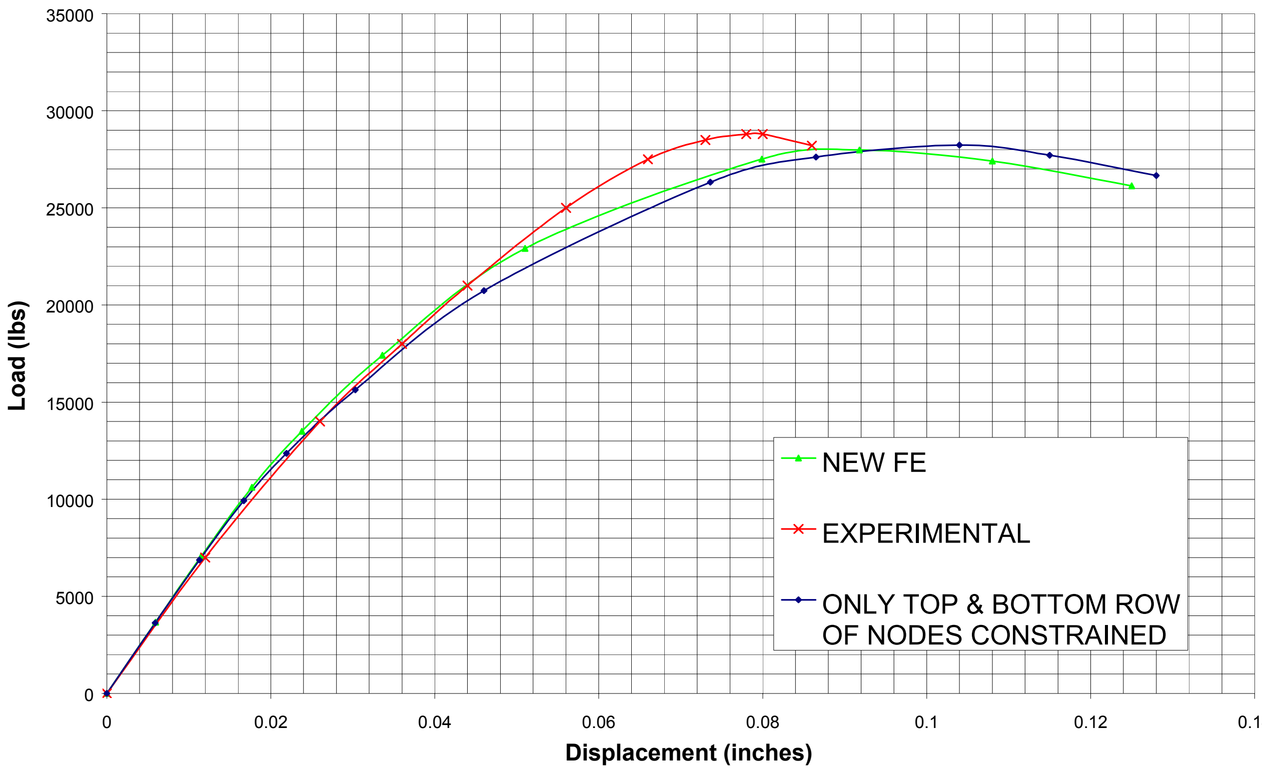

Figure 5. Load-Displacement of experimental panel and two FE shell models

3.3 Cerrobend solid elements

After examining the effects of various boundary conditions thoroughly, solid elements with Cerrobend properties were added to the top and bottom rows of elements in the FE model. It was thought that the solid elements would represent experimental end conditions more accurately than simply applying in plane constraints. Figures 6 and 7 show the first mode shapes of the buckled panel using solely shell elements with constraints to represent the Cerrobend, and shells combined with solid elements to represent the Cerrobend.

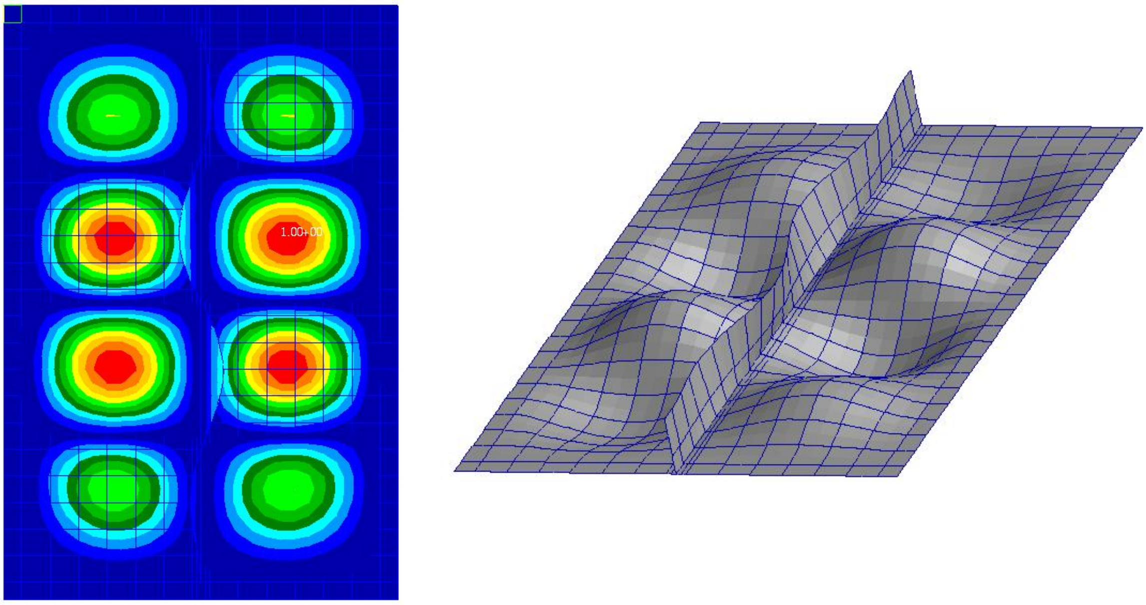

Figure 6. First mode shape of purely shell FE model

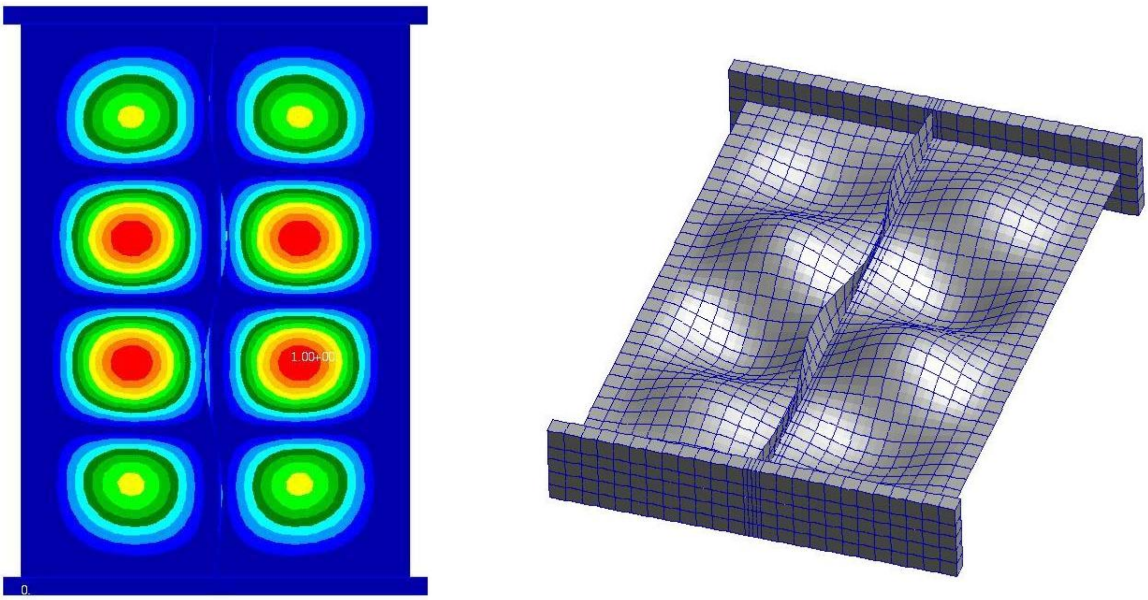

Figure 7. First mode shape of shell/solid FE model

The shapes are anti-symmetric, and would mirror one another if placed side by side. However, the deformation of the shell model is greater than that of the shell/solid model. The first eigenvalues for the shell model and shell/solid model are 0.35154 and 0.17190, respectively. Thus, the buckling load of the shell model is greater than that of the shell/solid model. This can be expected due to the stiffer boundary conditions on the purely shell model.

Load-deflection curves are plotted for the experimental panel, shell model, and shell/solid model in Figure 8. Stiffness and failure loads of the two FE models are compared to those of the experimental panel below in Figure 9.

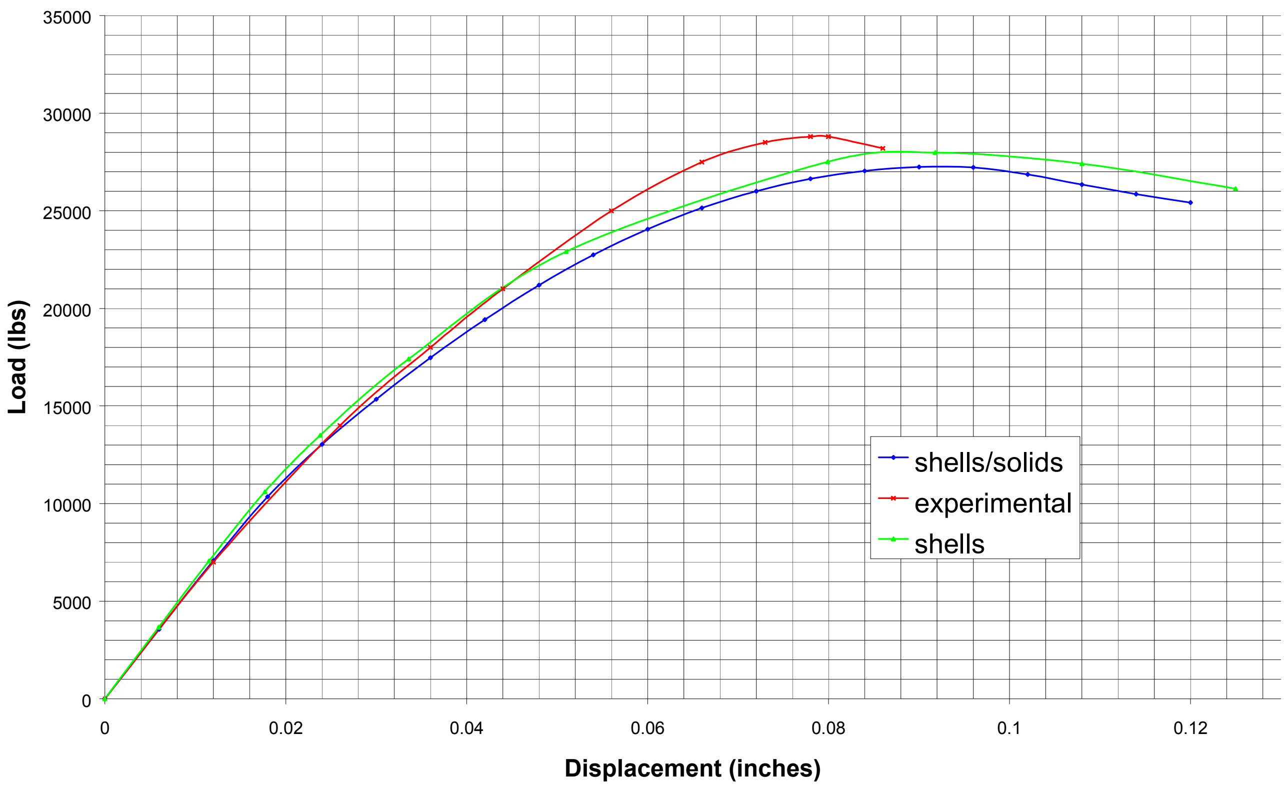

Figure 8. Load-Displacement of experimental panel and two FE models

Panel Type	**Stiffness (lbs/in)**	**% Diff**	**Failure Load (lbs)**	**% Diff**
Experimental Panel	593750	-------	28800	-------
Shell FE Model	611111	2.9	27983	2.8
Shell/Solid FE Model	593750	0	27242	5.4

Figure 9. Stiffness and failure loads of experimental panel and two FE models

As seen from the graph, the addition of solid elements to the panel model results in perfect correlation in elastic stiffness between the FE and experimental panel. The lower stiffness of the shell/solid model compared to the purely shell model is expected since the shell FE model was constrained completely at the top and bottom rows of elements, whereas the shell/solid model was constrained by the Cerrobend elements on each end. The material may have allowed slight movements out of plane, so the shell/solid model exhibited less stiff behaviour than the shell FE model. The shell/solid model under-predicts the failure load even more than the shell model, but is still relatively close to the experimental failure load, with only a 5.4% difference.

4 Conclusions and Future Work

To thoroughly examine the correlation of FE results with experimental results for a fuselage panel loaded in uni-axial compression, various FE models were analysed focusing on two major aspects:

(i) the shape of the panel being accurately modelled
(ii) the boundary conditions used to simulate experimental conditions

The first FE model was built solely with shell elements to represent the skin and stringer. Appropriate boundary conditions were applied to the panel edges to represent Cerrobend and steel bars, which held the panel in place in the experimental set-up. Previously, FE analysis had been done using an older version of ABAQUS, 5.8. Thus, the pad-up of the central welded section had to be modelled using a dummy layer with negligible stiffness. Version 6.1, currently in use, allows the element mid-surface to be offset from the geometry so that the shape of the panel could be modelled more accurately. Results showed a closer match-up in stiffness, though it was still over-predicted by FE analysis. However, the failure load was under-estimated, producing more conservative results.

Cerrobend boundary conditions were then varied to represent experimental conditions, but none matched better than using solid elements with Cerrobend material properties. This shell/solid model matched the experimental elastic stiffness perfectly. Both FE models under-predicted the failure load of the panel, and failure occurred at a greater displacement. However, both models were still within 5.4% of the experimental results.

For future experimental programmes, analysis will be undertaken to predict the length of Cerrobend needed to provide completely constrained ends of the fuselage panel when loaded in compression. Because of greater accuracy, solid elements will be used to represent the Cerrobend.

Having removed experimental errors dealing with panel constraints, the study can focus on additional modelling idealisation errors. Further investigation into the assumed width and material properties of the heat-affected zone will be carried out in the future.

References

[1] Gibson, A, "An investigation into the compressive strength and stability characteristics of welded aircraft fuselage panels", *PhD Thesis*, Queen's University of Belfast, July 2000.

[2] Lynch, C.J., Sterling, S.G., "A Finite Element Study of the Postbuckling Behaviour of a Flat Stiffened Panel", *ICAS Congress 2000*, Harrowgate, United Kingdom, paper no. ICAS-98-7,7,3.

[3] *ABAQUS Theory Manual*, Hibbit, Karlsson & Sorrenson, Inc., 2000.